3D Mapping of Vocal Fold Geometry During Articulatory Maneuvers Using Ultrashort Echo Time Imaging at 3.0 T

T. Frauenrath[1], A. Goemmel[2], C. Butenweg[2], M. Otten[3], and T. Niendorf[1,4]

[1]Berlin Ultrahigh Field Facility, Max-Delbrueck Center for Molecular Medicine, Berlin, Germany, [2]Chair of Structural Statics and Dynamics, RWTH, Aachen, Germany, [3]Erich-Thienhaus-Institute, Hochschule für Musik, Detmold, Germany, [4]Experimental and Clinical Research Center (ECRC), Charité Campus Buch, Humboldt-University, Berlin, Germany

Introduction:

Three-dimensional geometric data of the laryngeal anatomy are essential for biomechanical modeling of voice function. Traditional approaches of obtaining geometric data are two-dimensional approaches such as optical imaging (laryngoscopy) or *ex vivo* experiments. Although limited spatial insight can be obtained with stereoscopy imaging or hemi-larynx set-ups, three-dimensional *in vivo* measurements of vocal fold geometry are elusive hitherto. MRI is conceptually appealing for the pursuit of 3D laryngeal imaging since it affords sub-millimeter spatial resolution and versatile soft tissue/cartilage contrast. MRI comes with the penalty that it is not a real time approach. This constraint translates into stringent technical requirements in balancing scan time, image contrast, immunity to physiological motion, temporal resolution, and spatial resolution. Realizing these challenges and limitations this study uses a customized triggering scheme to synchronize high spatial resolution, ultrashort echo-time MRI with bulk or physiological motion with the ultimate goal of mapping vocal fold geometry during articulatory maneuvers including abduction and adduction.

Methods:

High frequency vocal fold oscillation is superimposed by bulk motion including abduction, adduction and swallowing. Compensation of this physiological motion was accomplished via sound presentation to the subject which guides phonation paralleled by external-triggering of the scanner as illustrated in Figure 1. For the latter a trigger waveform was delivered to the internal physiological signal controller circuitry of the MR scanner using the scanner's ECG input channel (Fig.1). To balance the competing constraints of signal-to-noise ratio (SNR) and imaging speed this study makes use of the SNR advantage inherent to high magnetic field strengths (3.0 T) in synergy with a 16-element coil array. The imaging protocol consisted of two series: (i) segmented, 3D gradient-echo imaging (FOV=(128x128) mm^2, matrix 256x256x80, TR=10.0 ms, TE=1.8 ms, flip angle=15°, acquired slice thickness=1 mm) and (ii) segmented, 3D ultra-short TE imaging (FOV=(128x128) mm^2, matrix=144x144x144, TE =0.14 ms, TR = 4.3 ms, flip angle = 5°) to avoid susceptibility artifacts at tissue and air interfaces. In vivo imaging on male and female subjects was conducted using a 3.0 T (Achieva, Philips, Best, The Netherlands). The subjects phonated in different pitches (modal and head register) and articulations. The articulations were chosen to be [m] and [e] to limit the effect of jaw motion during the measurements. 3D MRI data were included into segmentation to derive boundary conditions for finite-element models of vocal fold oscillation.

Results:

Different phonation states were imaged. For female subjects, 3D MRI data were recorded at a phonation pitch of 440 Hz in modal register with articulations of [m] and [e]. For male subjects, 3D MRI data were acquired for an: **(i)** [e] maneuver at a pitch of 220 Hz (modal register) and an **(ii)** [m] articulatory maneuver at pitches of 220 Hz and 440 Hz (head register). The Cartesian coordinate system of the segmented MRI data was reformatted so that the first axis was parallel to the vocal cords. The second axis was set perpendicular to the first axis following the head-feet direction so that the third axis resulted in the left-right direction. An example is depicted in Figure 2, which shows the contours of the oscillating vocal folds for an articulatory maneuver [e]. Vocal fold geometry was derived by identifying the boundaries at the tissue/air interface. For this purpose, polygonal curves were transformed into cubic splines as illustrated Figures 3 and Figure 4, which demonstrate differences in the vocal fold geometry for male and female subjects. Using articulations [e] and [m] at a head register (440 Hz) resulted in differences in the vocal fold geometry as shown in Fig. 5.

Discussion and Conclusions:

This work demonstrates the feasibility of three-dimensional MR imaging of vocal fold geometry which provides static and semi-dynamic training and reference data to be used in a finite-element model. Looking forward, this synergy between an imaging and computational approach offers several new insights into the anatomy and physiological mechanisms involved in human phonation. Further improvements are required to synchronize data acquisition with vocal fold oscillation. For this purpose, the subject's voice might serve as a triggering sound source for 3D-imaging of laryngeal tissues, vocal tract or other organs involved in speech and voice production. For example, electroglottography (EGG) might be ideal approach to synchronize MR data acquisition with vocal fold motion to reach the final goal of vocal fold oscillation imaging during speech production or singing. The move towards ultrahigh magnetic field strengths (7.0 T) in conjunction with the use of MR coil arrays tailored for laryngeal imaging offers further enhancements in spatial resolution, which hold the potential to provide benefits for 3D mapping of vocal fold geometry.

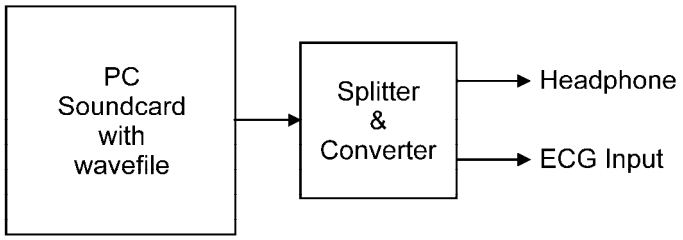

Figure 1: Basic synchronization scheme used for vocal fold geometry imaging. A fixed tone is supplied to the subject to guide articulatory maneuvers. Simultaneously, a virtual ECG waveform is sent to the scanners internal ECG unit, which initiates imaging. Imaging stops after a few seconds to insert a breathing period before another trigger is applied.

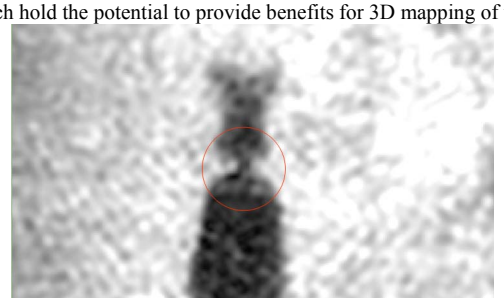

Figure 2: Contours of the oscillating vocal folds during articulation [e].

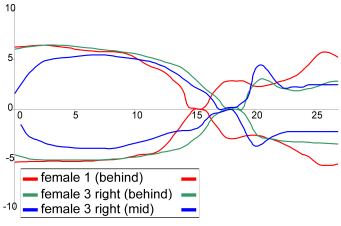

Figure 3: Comparison of vocal fold geometry for an articulatory maneuver [e] (marked in green and blue) and [m] (marked in red) in a female subject.

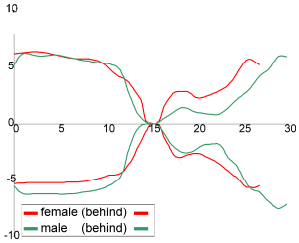

Figure 4: Comparison of vocal fold geometry derived from a female (red) and a male (green) subject both performing the articulatory maneuver [m].

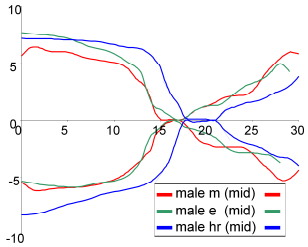

Figure 5: Vocal fold geometry derived from articulation [e] (green) and [m] (red) in a male subject using the head register (440 Hz).

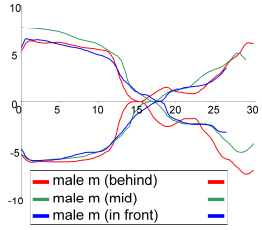

Figure 6: Comparison of different vocal fold geometries for positions along the anterior-posterior axis of a male subject with articulation [m] using modal register (220 Hz).